NANO LETTERS

2009
Vol. 9, No. 12
4467-4473

Nanocarrier Cross-Linking Density and pH Sensitivity Regulate Intracellular Gene Transfer

Jin-Oh You and Debra T. Auguste*

School of Engineering and Applied Sciences, Harvard University, Cambridge, Massachusetts 02138

Received August 25, 2009; Revised Manuscript Received October 5, 2009

ABSTRACT

Treatment of diseases on the molecular level by genetic material is limited by effective delivery mechanisms. We focused on the synthesis of a pH-sensitive gene delivery vehicle based on dimethylaminoethyl methacrylate (DMAEMA) with tunable swelling, cross-linking density, and DNA release kinetics within the endosomal pH range. Our strategy, which utilized a single step for DNA encapsulation, enhanced gene transfection efficiency and reduced cytotoxicity relative to polyethyleneimine (PEI) and poly-L-lysine (PLL).

The acidic endosomal compartment (pH 5−6[1,2] from early to late endosome) has been exploited in several drug and gene delivery applications.[3−7] PLL, PEI, and DMAEMA have been used extensively due to their high transfection efficiencies, but cytotoxicity often limits their clinical use.[8,9] pH-responsive liposomes incorporating dimethylammonium propane have been shown to be useful in delivery of short interfering RNA (siRNA).[10] The acidic endosome has also been used to mediate liposomal membrane fusion when palmitoylhomocysteine was incorporated.[11] In addition, core−shell nanoparticles incorporating pH-sensitive diethylaminoethyl methacrylate have been used to study cytosolic delivery for immunotherapy.[12] All of these strategies pay little attention to the rate and extent of changes in the endosome and how this may affect delivery. As illustrated in Figure 1, we optimized the vehicle design based on particle swelling and uptake, DNA release, gene transfection, and cytotoxicity.

DNA encoding for green fluorescent protein (GFP) was encapsulated within a series of pH-sensitive nanoparticles comprised of DMAEMA (a pH-sensitive monomer), 2-hydroxyethyl methacrylate (HEMA, a nonionic monomer), and tetraethylene glycol dimethacrylate (TEGDMA, a cross-linker). DMAEMA has a quaternizable tertiary amine that increases the cationic character of the drug delivery vehicle below its pK_a of 7.5,[13] resulting in electrostatic repulsion of ions in solution and volumetric swelling. We varied the DMAEMA/HEMA ratio (10/90, 20/80, or 30/70 mol/mol) and concentration of TEGDMA cross-linker (3, 6, or 9 mol %) to assess particles with a range of pH sensitivity and cross-linking density, respectively.

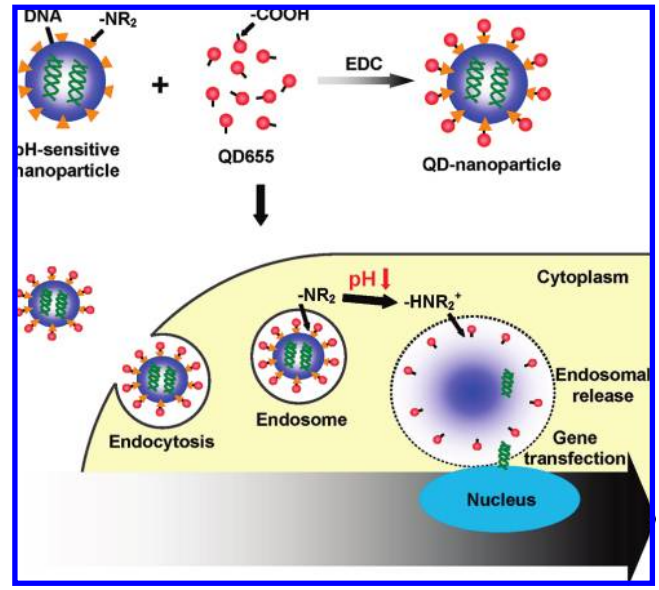

Figure 1. Schematic illustration of the synthesis and delivery of quantum-dot-labeled, pH-sensitive DMAEMA/HEMA nanoparticles encapsulating DNA.

DMAEMA/HEMA nanoparticles were synthesized by aqueous dispersion polymerization. Similar preparation of poly(HEMA) nanoparticles has been previously described[14−16] based on the insolubility of poly(HEMA) chains greater than 50 monomer units.[17] Addition of the cross-linker TEGDMA, initiators ammonium persulfate and sodium metabisulfite, and surfactant Pluronic F68 to a solution of DMAEMA and HEMA monomers resulted in the polymer-

* To whom correspondence should be addressed. Address: School of Engineering and Applied Sciences, Harvard University, 29 Oxford Street, Pierce 317, Cambridge, MA 02138. Tel: (617) 384-7980. Fax: (617) 495-9837. E-mail: auguste@seas.harvard.edu.

10.1021/nl902789s CCC: $40.75
Published on Web 10/20/2009

Table 1. Particle Size and Zeta Potential Analysis Of 10/90, 20/80, and 30/70 (mol/mol) DNA-Free DMAEMA/HEMA Nanoparticles Cross-linked with 3, 6, or 9 mol % TEGDMA and Naked DNA, PLL/DNA, and PEI/DNA Complexes in 10 mM TES Buffer

	diameter[d] (nm)	ζ potential[d] (mV)
naked DNA	57.6 ± 9.6	-8.9 ± 1.8
PLL/DNA	97.2 ± 12.3	18.1 ± 2.6
PEI/DNA	121.3 ± 10.1	24.8 ± 5.2
10/90[a]	197.2 ± 10.4	-18.6 ± 2.4
20/80[a]	201.8 ± 12.2	-13.5 ± 1.6
30/70[a]	203.4 ± 11.4	-10.3 ± 0.8
10/90[b]	196.5 ± 10.2	-16.6 ± 1.4
20/80[b]	197.6 ± 11.4	-14.8 ± 2.1
30/70[b]	201.2 ± 13.6	-10.4 ± 2.6
10/90[c]	195.4 ± 12.1	-14.6 ± 0.8
20/80[c]	196.8 ± 14.1	-11.2 ± 1.6
30/70[c]	200.2 ± 12.6	-8.7 ± 0.7

[a] Cross-linked with 3 mol % TEGDMA. [b] Cross-linked with 6 mol % TEGDMA. [c] Cross-linked with 9 mol % TEGDMA. [d] Data were performed in triplicate.

ization of homogeneous nanoparticles. The average size (Table 1) and morphology (Figure 2A) of nanoparticles were similar across the different DMAEMA/HEMA molar ratios and TEGDMA concentrations after synthesis. DMAEMA/HEMA nanoparticles were spherical and had a smooth surface morphology. Particles were, on average, 200 ± 21 nm in diameter and were not cytotoxic at a dose of 1.0 mg/mL (Figure 2B), significantly higher than other polycationic polymers used for gene transfection.[18] This size range accommodates systemic administration and passive delivery to tumors and sites of inflammation by the enhanced permeability and retention effect.[19]

We assessed the zeta potential (Table 1) of nanoparticles at pH 7.4 to describe the initial conditions under which particle uptake would occur. All formulations were initially negatively charged between -8.7 and -18.6 mV for 30/70 DMAEMA/HEMA cross-linked with 9 mol % TEGDMA and 10/90 DMAEMA/HEMA cross-linked with 3 mol % TEGDMA, respectively. DMAEMA partially hydrolyzes to methacrylic acid, which explains the negative zeta potential at the surface.[20] Increasing the DMAEMA content or the mol % of TEGDMA raised the zeta potential (all formulations remained negative). Our previous work showed that decreasing the pH, and thus protonating the DMAEMA group, increased the cationic character of the nanoparticles.[21]

The cationic DMAEMA was used to bind the GFP-encoding plasmid DNA (pDNA). The structural integrity of the pDNA encapsulated in DMAEMA/HEMA nanoparticles was examined by agarose gel electrophoresis (Figure 2C). The pDNA was extracted by incubating DMAEMA/HEMA nanoparticles in pH 5.5 phosphate buffer. Comparison of the naked pDNA (lane 2) with encapsulated pDNA (lane 6) confirmed that the DNA remained intact. Lanes 3−5 showed no presence of DNA in the supernatant after matrix polymerization. Judging from these results, we achieved almost 100% encapsulation of pDNA within our polymer matrixes and confirmed pDNA stability following DMAEMA/HEMA encapsulation.

Swelling of pH-sensitive DMAEMA/HEMA nanoparticles was observed at three monomer ratios (10/90, 20/80, and 30/70, Figure 2D), three concentrations of cross-linker (3, 6, and 9 mol % TEGDMA, Figure 2E), and five pHs (pH 5.5, 6.0, 6.5, 7.0, and 7.4; Figure S1, Supporting Information) as a function of time. The swelling ratio is defined as the average diameter of the swollen nanoparticles divided by the average diameter of the nanoparticle at pH 7.4. Higher swelling ratios were obtained by increasing the content of DMAEMA within the nanoparticle matrix. The 30/70 DMAEMA/HEMA nanoparticles had a significantly higher swelling ratio (2.0 ± 0.1) relative to the 10/90 (1.6 ± 0.1) and 20/80 (1.7 ± 0.1) formulations after 2 h at pH 5.5. Increasing the TEGDMA concentration resulted in a decrease in the swelling ratio. After 2 h of swelling, the swelling ratio of 30/70 DMAEMA/HEMA nanoparticles at pH 5.5 was 2.1 ± 0.2, 1.5 ± 0.2, and 1.2 ± 0.1 for 3, 6, and 9 mol % TEGDMA, respectively. Thus, we have shown that we can tune particle swelling by altering the DMAEMA content or cross-linking density.

To observe the extent of swelling, 30/70 DMAEMA/HEMA nanoparticles cross-linked with 3 mol % TEGDMA were swollen in pH 5.5, 6.0, 6.5, 7.0, and 7.4 phosphate buffers for 4 h. Particles at pH 7.4 exhibited a 20% increase after 2 h, whereas particles at pH 5.5 increased by 110%. At 2 h, the swelling ratios of DMAEMA/HEMA nanoparticles at pH 5.5, 6.0, 6.5, 7.0, and 7.4 were 2.1 ± 0.2, 1.8 ± 0.2, 1.6 ± 0.1, 1.4 ± 0.2, and 1.2 ± 0.1, respectively.

Encapsulating DNA decreased swelling of DMAEMA/HEMA nanoparticles by approximately 10%. DNA encapsulating 30/70 DMAEMA/HEMA nanoparticles cross-linked with 3 mol % TEGDMA were swollen in pH 5.5, 6.5, and 7.4 phosphate buffers for 4 h (Figure 2F). At pH 5.5, particle swelling after 2 h was 1.8 ± 0.2 (Figure 2F) and 2.0 ± 0.1 (Figure 2D) with and without DNA, respectively.

The swelling properties of HEMA have been extensively studied for a variety of chemical modifications.[22] Copolymerization of HEMA with hydrophilic monomers increases the swelling ratio, whereas polymerization of HEMA with increasing cross-linker concentration reduces its equilibrium swelling by reducing solvent diffusivity and relaxation of the polymer chains.[23] Equilibrium swelling occurs after approximately 2.5 h. Swelling is a function of water sorption and electrostatic interactions as a result of the protonated DMAEMA groups and the ions in solution. No swelling was measured above pH 8.0 (Figure S2, Supporting Information).

In addition to swelling, we observed that the cross-linking density was also affected by the formulation (Figure 3A). The Young's modulus, which did not change significantly with increasing DMAEMA content, more than doubled with increasing TEGDMA content. DMAEMA/HEMA hydrogels prepared with 3, 6, or 9 mol % TEGDMA had increasing moduli of 1.1 ± 0.1, 2.6 ± 0.3, and 6.3 ± 0.3 MPa, respectively. The DMAEMA/HEMA nanoparticles are elastomeric, similar in magnitude to synthetic rubber.[24]

Cross-linking density influenced particle uptake (Figure 3B). Particle uptake was quantified by the relative fluorescent intensity of quantum-dot-labeled particles sequestered within HeLa cells. Confocal microscopy sectioning revealed that

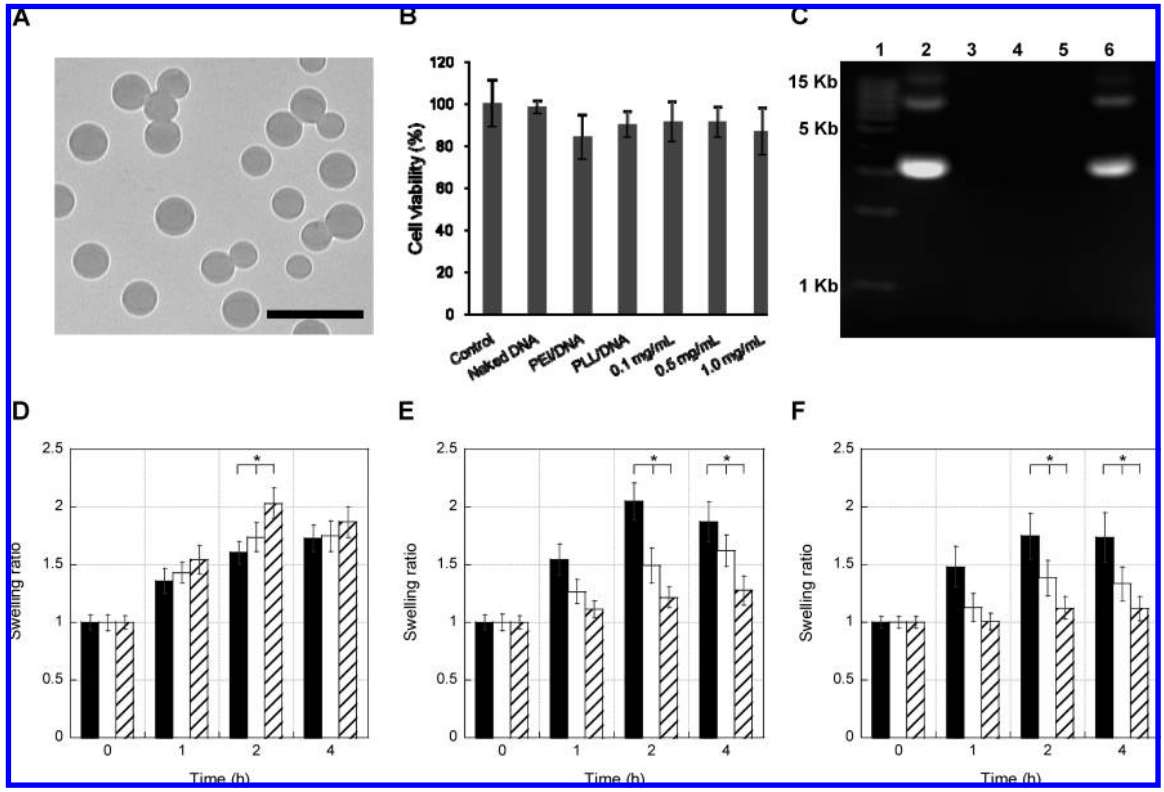

Figure 2. Particle characterization. (A) Transmission electron microscopy image of 30/70 (mol/mol) DMAEMA/HEMA nanoparticles cross-linked with 3 mol % TEGDMA. Scale bar = 500 nm. (B) Cell viability assay; 0.1, 0.5, and 1.0 mg of 30/70 (mol/mol) DMAEMA/HEMA nanoparticles cross-linked with 3 mol % TEGDMA were incubated with HeLa cells for 24 h and compared to a control without nanoparticles, naked DNA, PEI/DNA complexes ($N/P = 6$), and PLL/DNA complexes ($N/P = 2$). The error is the standard deviation from the mean, where $n = 3$. (C) Agarose gel electrophoresis for the assessment of plasmid DNA integrity extracted from 30/70 (mol/mol) DMAEMA/HEMA nanoparticles cross-linked with 3 mol % TEGDMA. Lane 1, EZ load 1 kb molecular ladder; lane 2, plasmid DNA; lane 3, supernatant after polymerization; lane 4, supernatant after first washing with pH 7.4 phosphate buffer; lane 5, supernatant after second washing with pH 7.4 phosphate buffer; lane 6, plasmid DNA extracted from nanoparticles. Volume swelling ratios of (*D*) 10/90 (black), 20/80 (white), and 30/70 (diagonal) (mol/mol) DMAEMA/HEMA nanoparticles cross-linked with 3 mol % TEGDMA at pH 5.5. (E) DMAEMA/HEMA (30/70, mol/mol) nanoparticles cross-linked with 3 (black), 6 (white), and 9 (diagonal) mol % TEGDMA at pH 5.5. (F) DNA encapsulating DMAEMA/HEMA (30/70, mol/mol) nanoparticles cross-linked with 3 mol % TEGDMA at pH 5.5 (black), 6.5 (white), and 7.4 (diagonal). The error is the standard deviation of the mean, where $n = 3$. *Statistical significance is calculated relative to pH 7.4 at a specific time point, $p < 0.01$.

the majority of nanoparticles were inside of cells not associating with the surface (Figure S3, Supporting Information). Particle uptake was not significantly affected by changes in the zeta potential based on increasing the DMAEMA content from 10 to 30 mol % (at 3 mol % TEGDMA, Figure S4, Supporting Information). Particle uptake was substantially impaired by more than two-fold by increasing the cross-linking density of the nanoparticles from 3 to 9 mol %. Over a period of 4 h, the uptake of quantum-dot-conjugated, 30/70 DMAEMA/HEMA nanoparticles cross-linked with 3 and 9 mol % TEGDMA was measured fluorimetrically (Figure 3B) or observed qualitatively (Figure 3C−J). Particle uptake increased with decreasing cross-linking density. After 4 h, 30/70 DMAEMA/HEMA nanoparticles had a fluorescence intensity of 153.1 ± 14.3 and 64.0 ± 6.7 for 3 and 9 mol % TEGDMA, respectively.

Visual confirmation of uptake is observed in successive confocal microscopy images, which show illumination of quantum-dot-labeled nanoparticles cross-linked with 3 mol % to appear earlier and in greater abundance. The first visual appearance of particle uptake was observed within the first hour for 3 mol % TEGDMA but not until 3 h for 9 mol % TEGDMA. At low cross-linking, particles were distributed throughout the cells. This is in contrast to highly cross-linked nanoparticles that have particles localized in the perinuclear region. Localization in the perinuclear region has been associated with sequestration within lysosomes[25] and with smaller diameter particles (<25 nm).[26]

A similar phenomenon of cross-linking density influencing particle uptake was observed using polyacrylamide beads. In contrast to our findings, Beningo et al.[27] found that macrophages increased the uptake of more rigid particles. Although they report that the measured Young's moduli were different by greater than three-fold, they did not report a magnitude for comparison to our results. In addition, the particle size was in the micrometer range, which also affects particle uptake. Further investigation into the response of specific cell types to cross-linking density may reveal a new method for cell targeting.

We have synthesized a series of pH-sensitive DMAEMA/HEMA nanoparticles with tunable swelling and cross-linking density (with similar size and zeta potential) to optimize gene

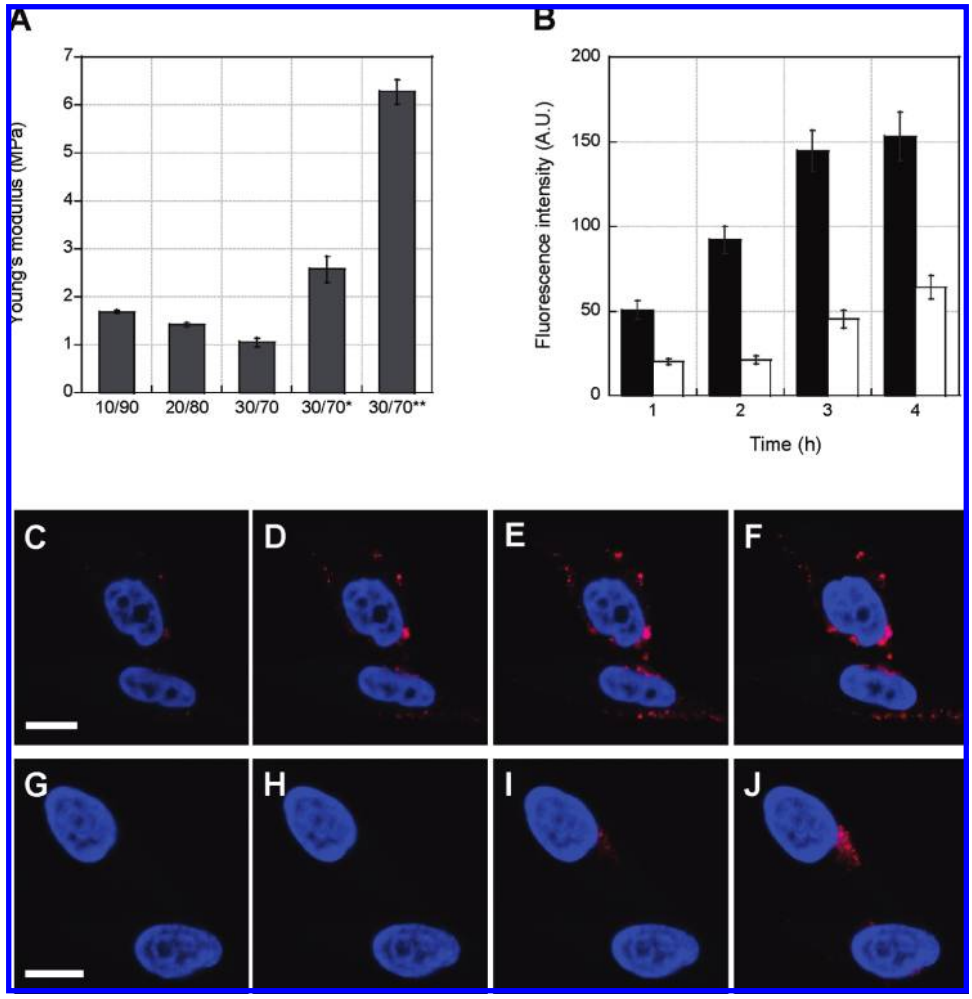

Figure 3. Elasticity of hydrogels and particle uptake. (A) Elastic moduli of different DMAEMA/HEMA ratios; $*$ = 6 mol % TEGDMA, and $**$ = 9 mol % TEGDMA. (B) Quantum-dot-conjugated DMAEMA/HEMA (30/70, mol/mol) nanoparticles cross-linked with 3 and 9 mol % TEGDMA are endocytosed by HeLa cells as a function of time (1, 2, 3, and 4 h incubations, respectively). The fluorescence intensity of uptaken particles cross-linked with 3 (black) and 9 mol % (white) TEGDMA was measured by a fluorescence microplate reader, and successive images were taken by confocal microscopy of (C−F) 3 and (G−J) 9 mol % TEGDMA at 1, 2, 3, and 4 h of transfection after addition of quantum-dot-conjugated particles. Both scale bars = 10 μm.

transfection efficiency. Transfection of HeLa cells by DMAEMA/HEMA nanoparticles was assessed for (1) a quantitative analysis of GFP expression as a function of time (Figure 4A and B) and (2) a qualitative assessment of GFP expression as a function of time (Figure S5A−F, Supporting Information). We quantified the extent of transfection by measuring relative fluorescence units (RFUs) of GFP-expressing HeLa cells at 0, 4, 12, 24, and 48 h (Figure 4A). For comparison, the transfection of HeLa cells was performed using naked pDNA and PLL/pDNA[28,29] and PEI/pDNA[4,30,31] complexes, which are known for their ability to enhance DNA transfection. PLL/pDNA and PEI/pDNA complexes were both positively charged, which contributes to their rapid association with the cell surface and subsequent uptake (Table 1).

We did not observe differences in transfection between pDNA complexes (PLL/pDNA and PEI/pDNA) and pDNA encapsulated within DMAEMA/HEMA nanoparticles at early times. However, at 24 and 48 h, the transfection of DMAEMA/HEMA nanoparticles was twice that of PLL/pDNA complexes and roughly 70% higher than PEI/pDNA complexes in the absence of serum (Figure 4A). GFP transfection was measured at 24 h to yield 6.9 ± 0.6, 7.4 ± 0.7, and 7.7 ± 0.6 RFUs for 10/90, 20/80, and 30/70 DMAEMA/HEMA nanoparticles, respectively. This was in comparison to PLL/pDNA and PEI/pDNA complexes that had measured transfection of 3.8 ± 0.5 and 5.4 ± 0.4 RFUs, respectively. In the presence of 10% serum (Figure S6, Supporting Information), gene transfection was enhanced by more than two-fold at 24 and 48 h by pDNA encapsulating DMAEMA/HEMA nanoparticles relative to polycation/pDNA complexes and naked pDNA. In comparison to nonresponsive HEMA particles (Figure S7, Supporting Information), pH-sensitive DMAEMA/HEMA nanoparticles enhanced gene transfection; this may be due to triggered DNA release and increased particle uptake.

Notably, the relative *N*/*P* ratio for the DMAEMA/HEMA nanoparticles (1.4 N/P for 10/90) was substantially lower than that for the PLL/pDNA and PEI/pDNA complexes. Reduction of the cationic character may reduce cytotoxicity. The overall transfection efficiency is not dependent on the monomer ratio of DMAEMA to HEMA; increasing DMAE-

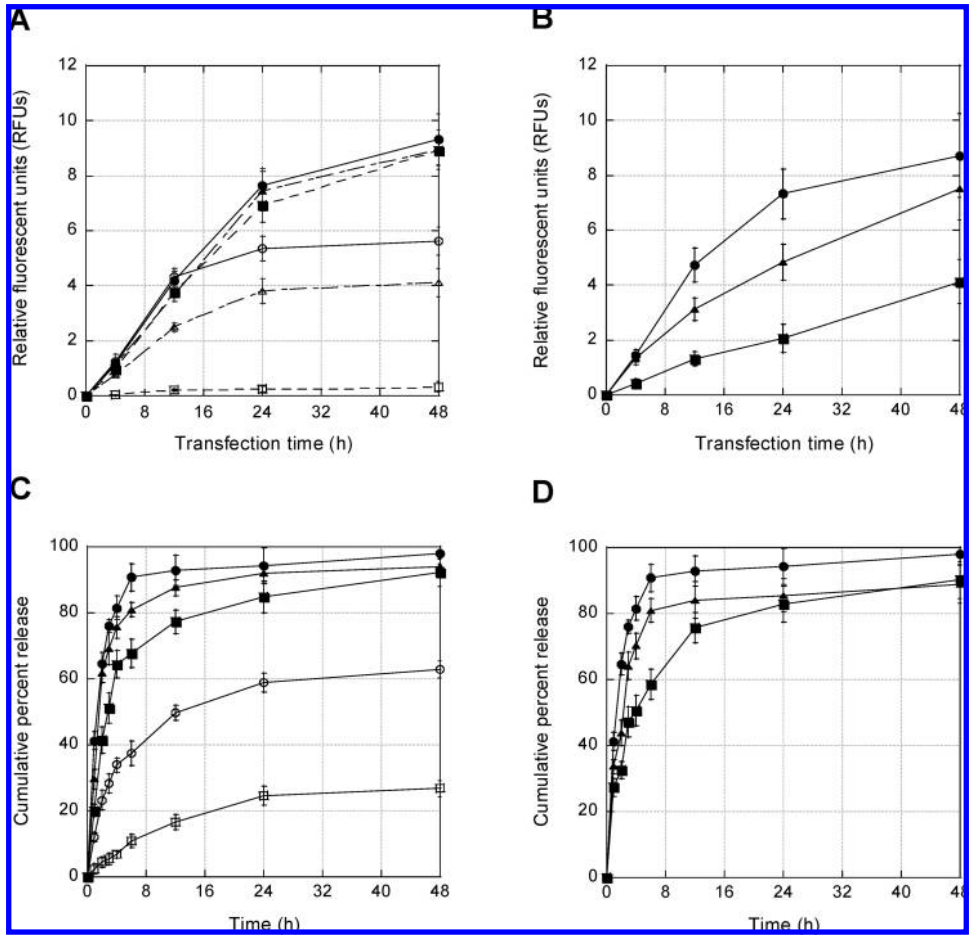

Figure 4. Gene transfection and controlled pDNA release. HeLa cells are treated separately with (A) 10/90 (■), 20/80 (▲), and 30/70 (●) (mol/mol) DMAEMA/HEMA nanoparticles cross-linked with 3 mol % TEGDMA encapsulating pDNA. Transfection with naked DNA (□), PLL/pDNA (Δ), and PEI/pDNA (○) complexes used as controls. (B) Transfection of HeLa cells treated separately with DMAEMA/HEMA (30/70, mol/mol) nanoparticles cross-linked with 3 (●), 6 (▲), and 9 (■) mol % TEGDMA encapsulating pDNA. The error is the standard deviation of the mean, where $n = 3$. Controlled pDNA release from (C) 10/90 (■), 20/80 (▲), and 30/70 (●) (mol/mol) DMAEMA/HEMA nanoparticles cross-linked with 3 mol % TEGDMA at pH 5.5. Also, pDNA release from 30/70 (mol/mol) DMAEMA/HEMA nanoparticles cross-linked with 6 (○) and 9 (□) mol % was obtained. Controlled pDNA release from (D) DMAEMA/HEMA (30/70, mol/mol) nanoparticles cross-linked with 3 mol % TEGDMA at pH 5.5 (●), 6.5 (▲), and 7.4 (■). The percentage of cumulative pDNA release was measured at 0, 1, 2, 3, 4, 6, 12, 24, and 48 h, respectively. The error is the standard deviation of the mean, $n = 3$.

MA above 10 mol % does not significantly increase gene transfection.

The effectiveness of DNA delivery was assessed by visual observation of GFP-expressing HeLa cells transfected with 30/70 DMAEMA/HEMA nanoparticles with 3 mol % TEGDMA (Figure S5A−F, Supporting Information). The images portray HeLa cells with a nuclei Hoescht stain merged with GFP expression and quantum-dot-conjugated nanoparticles. At 4 h, one-third of the cells are expressing GFP, which increases to two-thirds at 24 h.

Particle uptake was uniform for PLL/pDNA, PEI/pDNA, and DMAEMA/HEMA nanoparticles cross-linked with 3 mol % TEGDMA. Anionic nanoparticles may show increased uptake over cationic polymer/DNA complexes due to size differences.[32] Zahr et al. reported similar uptake between negatively and positively charged nanoparticles.[33]

Alternatively, we found that increasing the TEGDMA concentration modulated DNA transfection (Figure 4B). We assessed DNA transfection as a function of cross-linking density for 30/70 DMAEMA/HEMA nanoparticles at 3, 6, and 9 mol % TEGDMA. DMAEMA/HEMA nanoparticles showed significant DNA transfection, which was reduced with increasing cross-linking density. At equivalent particle uptake (comparison of 30/70 DMAEMA/HEMA nanoparticles cross-linked with 3 and 9 mol % after 1 and 3 h incubation), DNA transfection is still hindered by DNA release (Figure 4B).

Controlled release of pDNA from the pH-sensitive nanoparticles showed a dependence on the DMAEMA content, cross-linker concentration, and solvent pH (Figure 4C and D). The percentage of pDNA released after 6 h at pH 5.5 was 67.8 ± 4.3, 80.9 ± 2.2, and 90.8 ± 4.1% for 10/90, 20/80, and 30/70 DMAEMA/HEMA nanoparticles cross-linked with 3 mol % TEGDMA, respectively. When the TEGDMA concentration was increased, pDNA release was significantly decreased. The percentage of pDNA released after 6 h from 30/70 DMAEMA/HEMA nanoparticles at pH 5.5 was 90.8 ± 4.1, 37.5 ± 3.6, and 11.0 ± 2.0% for 3, 6, and 9 mol % TEGDMA, respectively. pDNA release was also observed as a function of pH. The percentage of pDNA

released after 6 h from 30/70 DMAEMA/HEMA nanoparticles cross-linked with 3 mol % TEGDMA was 68.7 ± 3.1, 61.2 ± 2.7, and 44.3 ± 3.5% at pH 5.5, 6.5, and 7.4, respectively. Nanoparticles with higher swelling (based on DMAEMA content and cross-linking density) exhibited greater transfection and faster DNA release.

pDNA release was not reduced at higher DMAEMA content (Figure 4C). Faster pDNA release occurred with 30/70 rather than 10/90 DMAEMA/HEMA nanoparticles cross-linked with 3 mol % TEGDMA. This suggests that the pDNA is not bound tightly with the cationic DMAEMA units and that matrix swelling controls the release rate.

Clearly, there are molecular interactions that control the release rate, which include hydrogen bonding, physical cross-links, and hydrophobic and electrostatic interactions. Our tentative picture is that the pDNA is entrained within a pH-sensitive polymer network. pDNA release and swelling is a function of the expansion of the pH-sensitive network, which is regulated by the DMAEMA content, cross-linking density (mol % TEGDMA), and solution pH.

Our results suggest that we have a semi-interpenetrating network (SIPN) where negatively charged pDNA is interlaced within a DMAEMA-co-HEMA polymer network. We observed degradation of these networks on the order of 1 to 3 days; this may result from physical precipitation of polyHEMA units that form physical cross-links in the particle structure. Stimuli-responsive SIPN networks prepared from *N*-isopropylacrylamide and chitosan showed similar swelling characteristics, where swelling decreases with increasing cross-linking density and increasing chitosan content.[34] Swelling plateaued after 4 h.

Molecule release is described as a function of time t by a power law model presented as $M_t = M_\infty t^n$, where M_t and M_∞ are the respective masses of molecule release at time t and infinity and n is the diffusion exponent.[35] Information about the release mechanism can be gained by fitting the molecule release data and comparing the value of n to the semiempirical values reported by Peppas.[35] The data from the release curves in Figure 4C were fitted to the power law equation. The fitted diffusion exponent n was found to be 0.34, 0.24, and 0.19 for 10/90, 20/80, and 30/70 DMAEMA/HEMA ratios cross-linked with 3 mol % TEGDMA, respectively. This implies that Fickian diffusion plays an important role in DNA release from DMAEMA/HEMA nanoparticles. At higher cross-linking density, DNA release is governed by anomalous (non-Fickian) diffusion. The fitted diffusion exponent n was 0.40 and 0.65 for 30/70 DMAEMA/HEMA nanoparticles cross-linked with 6 and 9 mol % TEGDMA, respectively.

In summary, DMAEMA/HEMA nanoparticles are nontoxic, encapsulate nearly 100% DNA, and are prepared in a simple, inexpensive, one-step procedure. Enhanced transfection is attributed to particle uptake, endosomal swelling of DMAEMA/HEMA nanoparticles, and subsequent delivery of the DNA via diffusion through a swollen network. The pH-sensitive DMAEMA/HEMA nanoparticles are efficient gene carriers in comparison with traditional methods which rely on pDNA condensation with PLL or PEI without the drawback of cytotoxicity.

Acknowledgment. The authors would like to thank Robert K. Prud'homme and Stephen P. Armes for helpful discussions. This work was performed in part at the Center for Nanoscale Systems (CNS), a member of the National Nanotechnology Infrastructure Network (NNIN), which is supported by the National Science Foundation under NSF Award No. ECS-0335765. CNS is part of the Faculty of Arts and Sciences at Harvard University.

Supporting Information Available: Methods and materials. This material is available free of charge via the Internet at http://pubs.acs.org.

References

(1) Presley, J. F.; Mayor, S.; Dunn, K. W.; Johnson, L. S.; Mcgraw, T. E.; Maxfield, F. R. *J. Cell Biol.* **1993**, *122* (6), 1231–1241.
(2) Aniento, F.; Gu, F.; Parton, R. G.; Gruenberg, J. *J. Cell Biol.* **1996**, *133* (1), 29–41.
(3) Medina-Kauwe, L. K.; Xie, J.; Hamm-Alvarez, S. *Gene Ther.* **2005**, *12* (24), 1734–1751.
(4) Boussif, O.; Lezoualc'h, F.; Zanta, M. A.; Mergny, M. D.; Scherman, D.; Demeneix, B.; Behr, J. *Proc. Natl. Acad. Sci. U.S.A.* **1995**, *92* (16), 7297–7301.
(5) Haensler, J.; Szoka, F. C. *Bioconjug. Chem.* **1993**, *4* (5), 372–379.
(6) Abdallah, B.; Hassan, A.; Benoist, C.; Goula, D.; Behr, J. P.; Demeneix, B. A. *Gene Ther.* **1996**, *7* (16), 1947–1954.
(7) Ros, C.; Burckhardt, C. J.; Kempf, C. *J. Virol.* **2002**, *76* (24), 12634–12645.
(8) Boeckle, S.; von Gersdorff, K.; van der Piepen, S.; Culmsee, C.; Wagner, E.; Ogris, M. *J. Gene Med.* **2004**, *6* (10), 1102–1111.
(9) Cherng, J. Y.; vandeWetering, P.; Talsma, H.; Crommelin, D. J. A.; Hennink, W. E. *Pharm. Res.* **1996**, *13* (7), 1038–1042.
(10) Auguste, D. T.; Furman, K.; Wong, A.; Fuller, J.; Armes, S. P.; Deming, T. J.; Langer, R. *J. Controlled Release* **2008**, *130* (3), 266–274.
(11) Connor, J.; Yatvin, M. B.; Huang, L. *Proc. Natl. Acad. Sci. U.S.A.* **1984**, *81* (6), 1715–1718.
(12) Hu, Y.; Litwin, T.; Nagaraja, A. R.; Kwong, B.; Katz, J.; Watson, N.; Irvine, D. J. *Nano Lett.* **2007**, *7* (10), 3056–3064.
(13) van de Wetering, P.; Moret, E. E.; Schuurmans-Nieuwenbroek, N. M. E.; van Steenbergen, M. J.; Hennink, W. E. *Bioconjug. Chem.* **1999**, *10* (4), 589–597.
(14) Klaus, T.; Imroz Ali, A. M.; Sedlak, M. *Colloid Polym. Sci.* **2005**, *283* (4), 351–358.
(15) Okubo, M.; Yamamoto, Y.; Kamei, S. *Colloid Polym. Sci.* **1989**, *267* (10), 861–865.
(16) Chu, H. H.; Fu, D. C. *Macromol. Rapid Commun.* **1998**, *19* (2), 107–110.
(17) Weaver, J. V. M.; Bannister, I.; Robinson, K. L.; Bories-Azeau, X.; Armes, S. P.; Smallridge, M.; McKenna, P. *Macromolecules* **2004**, *37* (7), 2395–2403.
(18) Putnam, D.; Gentry, C. A.; Pack, D. W.; Langer, R. *Proc. Natl. Acad. Sci. U.S.A.* **2001**, *98* (3), 1200–1205.
(19) Brannon-Peppas, L.; Blanchette, J. O. *Adv. Drug Delivery Rev.* **2004**, *56* (11), 1649–1659.
(20) van de Wetering, P.; Cherng, J. Y.; Talsma, H.; Crommelin, D. J. A.; Hennink, W. E *J. Controlled Release* **1998**, *53* (1−3), 145–153.
(21) You, J. O.; Auguste, D. T. *Biomaterials* **2008**, *29* (12), 1950–1957.
(22) Bako, J.; Szepesi, M.; Veres, A. J.; Cserhati, C.; Borbely, Z. M.; Hegedus, C.; Borbely, J. *Colloid Polym. Sci.* **2008**, *286* (3), 357–363.
(23) Kabra, B. G.; Gehrke, S. H.; Hwang, S. T.; Ritschel, W. A. *J. Appl. Polym. Sci.* **1991**, *42* (9), 2409–2416.
(24) Flory, P. J. *Chem. Rev.* **1944**, *35* (1), 51–75.
(25) Swanson, J. A.; Locke, A.; Ansel, P.; Hollenbeck, P. J. *J. Cell Sci.* **1992**, *103* (1), 201–209.
(26) Laia, S. K.; Hidab, K.; Mana, S. T.; Chena, C.; Machamerf, C.; Schroerc, T. A.; Hanes, J. *Biomaterials* **2007**, *28* (18), 2876–2884.
(27) Beningo, K. A.; Wang, Y. *J. Cell Sci.* **2002**, *115* (4), 849–856.
(28) Mislick, K. A.; Baldeschwieler, J. D. *Proc. Natl. Acad. Sci. U.S.A.* **1996**, *93* (22), 12349–12354.

(29) Ferkol, T.; Perales, J. C.; Mularo, F.; Hanson, R. W. *Proc. Natl. Acad. Sci. U.S.A.* **1996**, *93* (1), 101–105.
(30) Orson, F. M.; Song, L.; Gautam, A.; Densmore, C. L.; Bhogal, B. S.; Kinsey, B. M. *Gene Ther.* **2002**, *9* (7), 462–471.
(31) Suh, J.; Wirtz, D.; Hanes, J. *Proc. Natl. Acad. Sci. U.S.A.* **2003**, *100* (7), 3878–3882.
(32) Win, K. Y.; Feng, S. S. *Biomaterials* **2005**, *26* (15), 2713–2722.
(33) Zahr, A. S.; Davis, C. A.; Pishko, M. V. *Langmuir* **2006**, *22* (19), 8178–8185.
(34) Lee, W. F.; Chen, Y. J. *J. Appl. Polym. Sci.* **2001**, *82* (10), 2487–2496.
(35) Ritger, P. L.; Peppas, N. A. *J. Controlled Release* **1987**, *5* (1), 37–42.

NL902789S